

The Sedimentation Scour Model in *FLOW-3D*

Gengsheng Wei, James Brethour, Markus Grünzner and Jeff Burnham

August 2014; Revised October 2014

1. Introduction

The three-dimensional sediment scour model for non-cohesive soils was first introduced to *FLOW-3D* in Version 8.0 to simulate sediment erosion and deposition (Brethour, 2003). It was coupled with the three-dimensional fluid dynamics and considered entrainment, drifting and settling of sediment grains. In Version 9.4 the model was improved by introducing bedload transport and multiple sediment species (Brethour and Burnham, 2010). Although applications were successfully simulated, a major limitation of the model was the approximate treatment of the interface between the packed and suspended sediments. The packed bed was represented by scalars rather than FAVOR™ (Fractional Area Volume Obstacle Representation, the standard treatment for solid components in *FLOW-3D*). As a result, limited information about the packed bed interface was available. That made accurate calculation of bed shear stress, a critical factor determining the model accuracy, challenging.

In this work, the 3D sediment scour model is completely redeveloped and rewritten. The model is still fully coupled with fluid flow, allows multiple non-cohesive species and considers entrainment, deposition, bedload transport and suspended load transport. The fundamental difference from the old model is that the packed bed is described by the FAVOR™ technique. At each time step, area and volume fractions describing the packed sediments are calculated throughout the domain. In the mesh cells at the bed interface, the location, orientation and area of the interface are calculated and used to determine the bed shear stress, the critical Shields parameter, the erosion rate and the bedload transport rate. Bed shear stress is evaluated using the standard wall function with consideration of bed surface roughness that is related to the median grain size d_{50} . A sub-mesh method is developed and implemented to calculate bedload transport. Computation of erosion considers entrainment and deposition simultaneously in addition to bedload transport. The settling velocity of grains is calculated using an existing equation to account for deposition and transport of the suspended sediments.

Furthermore, a shallow-water sediment scour model is developed in this work by adapting the new 3D model. It is coupled with the 2D shallow water flows to calculate depth-averaged properties for both suspended and packed sediments. Its main difference from the 3D model is that the turbulent bed shear stress is calculated using a well-accepted quadratic law rather than the log wall function. The drag coefficient for the bed shear stress is either user-given or locally evaluated using the water depth and the bed surface roughness that is proportional to d_{50} of the bed material.

With this model, users can only use one geometry component to define the initial packed sediment region. The component, however, can be composed of multiple geometry subcomponents with different fractions of sediment species. If no packed bed exists initially, a geometry component is automatically generated by the code to represent the packed bed when it is formed during simulation.

2. Sediment Theory

The sediment scour model assumes multiple sediment species with different properties including grain size, mass density, critical shear stress, angle of repose and parameters for entrainment and transport. For example, medium sand, coarse sand and fine gravel can be categorized into three different species in a simulation. The model calculates all the sediment transport processes including bedload transport, suspended load transport, entrainment and deposition for each species.

Entrainment is the process by which turbulent eddies remove the grains from the top of the packed bed and carry them into suspension. It occurs when the bed shear stress exceeds a threshold value (critical shear stress). After entrained, the grains are carried by the water current within a certain height above the packed bed, known as the *suspended load transport*. *Deposition* takes place when suspended grains settle onto the packed bed due to the combined effect of gravity, buoyancy and friction. *Bedload transport* describes the rolling, hopping and sliding motions of grains along the packed bed surface in response to the shear stress applied by fluid flow.

2.1 Bed shear stress

The bed shear stress is the shear stress applied by fluid on the packed bed surface. It is calculated using the wall function for 3D turbulence flows,

$$u = u_\tau \left[\frac{1}{\kappa} \ln \left(\frac{Y}{\frac{\nu}{u_\tau} + k_s} \right) \right] \quad (1)$$

where u_τ is the shear velocity, $u_\tau = \sqrt{\tau/\rho}$, τ is the bed shear stress, ρ is the bulk density of the fluid-sediment mixture, Y is the distance from the wall, ν is the kinematic viscosity of the bulk flow, $\kappa = 0.4$ is the Von Karman constant, k_s is the Nikuradse roughness. In this model, k_s is related to grain size as

$$k_s = c_s d_{50} \quad (2)$$

where d_{50} is the median grain diameter of the bed material, and c_s is a user-definable coefficient. The recommended value of c_s is 2.5.

In shallow water flows, the quadratic friction law is used to evaluate the bed shear stress,

$$\tau = \rho_f C_D \bar{v} |\bar{v}| \quad (3)$$

where \bar{v} is the depth-averaged fluid velocity, ρ_f is the fluid density, and C_D is the drag coefficient that can be either prescribed by users (default value is 0.0026) or locally determined in terms of the roughness k_s (Soulsby, 1997),

$$C_D = \left[\frac{\kappa}{B + \ln(z_0/h)} \right]^2 \quad (4)$$

with h as the local water depth, $B=0.71$, and $z_0 = k_s/30$.

2.2 Critical Shields parameter

The Shields parameter is a dimensionless form of bed shear stress defined as

$$\theta_n = \frac{\tau}{g d_n (\rho_n - \rho_f)} \quad (5)$$

where g is gravity in absolute value, ρ_n is the mass density of sediment grains, and d_n is grain diameter. The subscript n represents the n -th sediment species.

The critical Shields parameter $\theta_{cr,n}$ is used to define the critical bed shear stress $\tau_{cr,n}$, at which sediment movement begins for both entrainment and bedload transport,

$$\theta_{cr,n} = \frac{\tau_{cr,n}}{g d_n (\rho_n - \rho_f)} \quad (6)$$

The base value of $\theta_{cr,n}$ is for a flat and horizontal bed of identically-sized grains. It can be either specified by users (0.05 by default) or determined from the Soulsby-Whitehouse equation (Soulsby and Whitehouse, 1997),

$$\theta_{cr,n} = \frac{0.3}{1 + 1.2 d_{*,n}} + 0.055(1 - e^{-0.02 d_{*,n}}) \quad (7)$$

where $d_{*,n}$ is the dimensionless grain size given by

$$d_{*,n} = d_n \left[\frac{g(s_n - 1)}{\nu_f^2} \right]^{1/3} \quad (8)$$

Here $s_n = \rho_n/\rho_f$, and ν_f is the kinematic viscosity of fluid. Note the Soulsby-Whitehouse equation in equation (7) has replaced the Shields-Rouse equation used in the old model due to its wider range of validity (Soulsby, 1997).

At a sloping bed interface, the gravity applies a tangential component of force to make the packed bed more or less stable depending on the flow direction. As a result, the

critical shear stress increases if the fluid flow goes up the slope and decreases if the flow goes down. It is an option to users that $\theta_{cr,n}$ can be modified for the sloping bed effect following Soulsby (1997),

$$\theta'_{cr,n} = \theta_{cr,n} \frac{\cos\psi \sin\beta + \sqrt{\cos^2\beta \tan^2\phi_n - \sin^2\psi \sin^2\beta}}{\tan\phi_n} \quad (9)$$

where β is the slope angle of the packed bed, ϕ_n is the angle of repose defined as the steepest slope angle before grains slide by themselves (default values is 32°), and ψ is the angle between the upslope direction and the fluid flow adjacent to the sloping bed, as shown in Figure 1. ψ ranges between 0° and 180° , with 0° corresponding to up-slope flow and 180° down-slope flow.

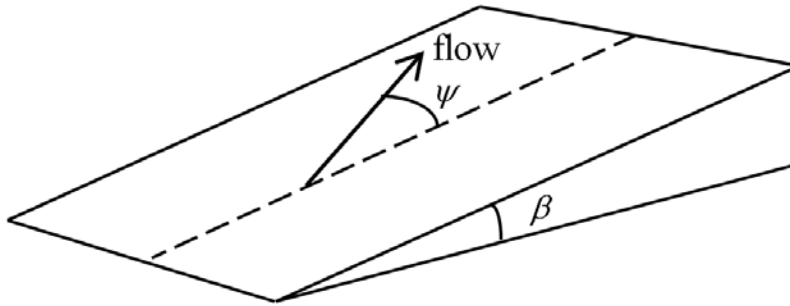


Figure 1. Sloping bed and flow direction

2.5. Entrainment and Deposition

In this model, entrainment and deposition are treated as two opposing micro-processes that take place at the same time. They are combined to determine the net rate of exchange between packed and suspended sediments. For entrainment, the velocity at which the grains leave the packed bed is the lifting velocity and is calculated based on Winterwerp et al. (1992),

$$\mathbf{u}_{lift,n} = \mathbf{n}_b \alpha_n d_{*,n}^{0.3} (\theta_n - \theta_{cr,n})^{1.5} \sqrt{g d_n (s_n - 1)} \quad (10)$$

where α_n is the entrainment coefficient of species n (default value is 0.018), and \mathbf{n}_b is the outward normal vector of the packed bed surface. In deposition, the settling velocity of Soulsby (1997) is used,

$$\mathbf{u}_{settle,n} = \frac{\mathbf{g}}{g} \left[(10.36^2 + 1.049 d_{*,n}^3)^{1/2} - 10.36 \right] \frac{v_f}{d_n} \quad (11)$$

where \mathbf{g} is the gravity acceleration. $\mathbf{u}_{settle,n}$ is assumed in the same direction of \mathbf{g} .

2.3. Bedload Transport

The dimensionless form of the bedload transport rate for species n is defined as

$$\Phi_n = \frac{q_{b,n}}{[g(s_n - 1)d_n^3]^{\frac{1}{2}}} \quad (12)$$

where $q_{b,n}$ is the volumetric bedload transport rate per unit bed width (in units of volume per width per time). Φ_n is calculated using the Meyer-Peter and Muller equation (1948),

$$\Phi_n = B_n(\theta_n - \theta_{cr,n})^{1.5} c_{b,n} \quad (13)$$

where B_n is the bedload coefficient. It is generally 5.0 to 5.7 for low transport, around 8.0 for intermediate transport, and up to 13.0 for very high transport (for example, sand in sheet flow under waves and currents). The default value used in **FLOW-3D** is 8.0, which is the most commonly used value in the literature. $c_{b,n}$ is the volume fraction of species n in the bed material,

$$c_{b,n} = \frac{\text{net volume of species } n}{\text{net volume of all species}} \quad (14)$$

and satisfies

$$\sum_{n=1}^N c_{b,n} = 1.0 \quad (15)$$

where N is the total number of species. Note $c_{b,n}$ does not exist in the original Meyer-Peter and Muller equation. It is added in equation (13) to account for the effect of multiple species.

The relationship in Van Rijn (1984) is used to estimate the bedload layer thickness h_n ,

$$h_n = 0.3d_n d_{*,n}^{0.7} \left(\frac{\theta_n}{\theta_{cr,n}} - 1 \right)^{0.5} \quad (16)$$

The bedload velocity $\mathbf{u}_{b,n}$ is calculated by

$$\mathbf{u}_{b,n} = \frac{\mathbf{q}_{b,n}}{h_n c_{b,n} f_b} \quad (17)$$

where f_b is the total packing fraction of sediments. Both $\mathbf{u}_{b,n}$ and $\mathbf{q}_{b,n}$ are in direction of the fluid flow adjacent to the bed interface.

2.5. Suspended load transport

For each species, the suspended sediment concentration is calculated by solving its own transport equation,

$$\frac{\partial C_{s,n}}{\partial t} + \nabla \cdot (C_{s,n} \mathbf{u}_{s,n}) = \nabla \cdot \nabla (DC_{s,n}) \quad (18)$$

Here $C_{s,n}$ is the suspended sediment mass concentration, which is defined as the sediment mass per volume of fluid-sediment mixture; D is the diffusivity; $\mathbf{u}_{s,n}$ is the sediment velocity of species n . It is noted that each sediment species in suspension moves at its own velocity that is different from those of fluid and other species. This is because grains with different mass density and sizes have different inertia and receive different drag force.

Correspondingly, the suspended sediment volume concentration $c_{s,n}$ is defined as the suspended sediment species n volume per volume of fluid-sediment mixture. It is related to $C_{s,n}$ by

$$c_{s,n} = \frac{C_{s,n}}{\rho_n} \quad (19)$$

The mass density of the fluid-sediment mixture is calculated using

$$\bar{\rho} = \sum_{m=1}^N c_{s,m} \rho_{s,m} + (1 - c_{s,tot}) \rho_f \quad (20)$$

where $c_{s,tot}$ is the total suspended sediment volume concentration,

$$c_{s,tot} = \sum_{m=1}^N c_{s,m} \quad (21)$$

To solve equation (18) for $C_{s,n}$, $\mathbf{u}_{s,n}$ must be calculated first. It is assumed that: 1) the grains in suspension do not have strong interactions with each other; 2) the velocity difference between the suspended sediments and the fluid-sediment mixture is mainly the settling velocity of grains, $\mathbf{u}_{settle,n}$, that is defined in equation (11). Thus, $\mathbf{u}_{s,n}$ is evaluated using

$$\mathbf{u}_{s,n} = \bar{\mathbf{u}} + \mathbf{u}_{settle,n} c_{s,n} \quad (22)$$

where $\bar{\mathbf{u}}$ is the bulk velocity of the fluid-sediment mixture,

$$\bar{\mathbf{u}} = \sum_{m=1}^N c_{s,m} \mathbf{u}_{s,m} + (1 - c_{s,tot}) \mathbf{u}_f \quad (23)$$

In *FLOW-3D*, $\bar{\mathbf{u}}$ is obtained by solving the continuity and Navier-Stokes equations with a turbulence closure model.

3. Model Validation and Applications

1) Sediment deposition in a tank

Figure 2 shows the experimental setup of Gladstone et al (1998). The experiment was performed in a long rectangular tank with one end separated from the remainder by a lockgate, behind which sediment is held uniformly in suspension until the lockgate is raised. The experiment began with the raising of the lock gate, and the resulting density current caused the sediment to distribute along the length of the tank. The distribution of the sediment was measured, although the ratio of the sediment species in the deposited bed was not. The experiment was repeated for seven cases, each case with a different ratio of coarse to fine sediment. The sediments used had a diameter of 25 μm and 69 μm for the fine and coarse sediments, respectively. Both sediments were silicon carbide particles and had a microscopic density of 3.217g/cm³.

The experiment was simulated with *FLOW-3D*. The sedimentation and scour model was used with sediment diameter and density specified and all other settings left to default. The output was converted into deposition density which is mass of sediments per unit area along the bottom of the tank and is compared directly to the experimental results. Table 1 lists the cases that had been both conducted experimentally and simulated. All simulations were conducted on a three-dimensional single mesh block with 105,600 uniform cells, each about a 1.9cm cube.

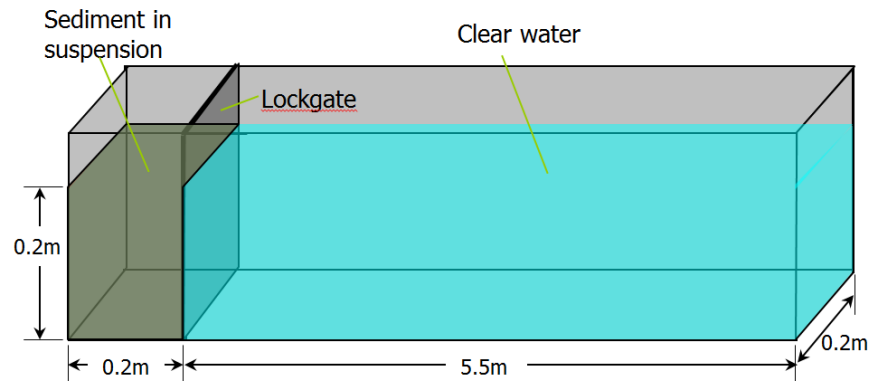


Figure 2. Experimental tank emulated by the simulation. The sediment in suspension moves into the remainder of the tank when the lockgate is lifted.

	Fine grains (25 μm)	Coarse grains (69 μm)
Case 1	0%	100%
Case 2	50%	50%
Case 3	100%	0%

Table 1. The cases that were run using the sedimentation tank described in Figure 2.

Figure 3 shows the measured and simulated deposit density after the flow-front has completed its advance and all sediment had settled. It is seen that the trend, the maximum and minimum values of deposit density and the final location of the flow-front are predicted well by the simulations, although the deposit density is underestimated before its peak value location and overestimated after that to some degrees.

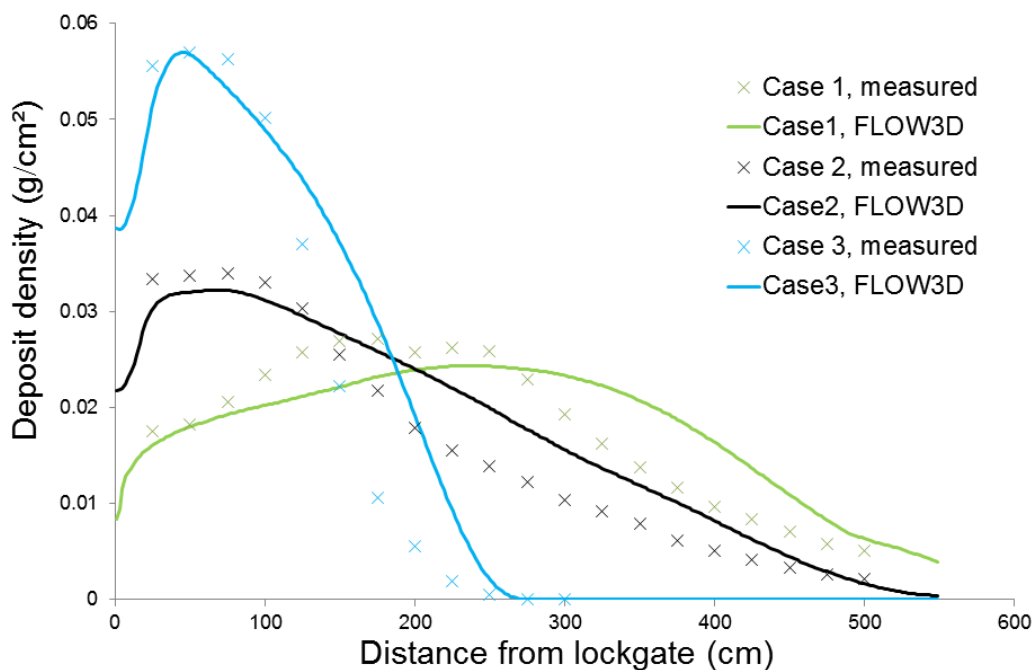


Figure 3. Plots of deposit density from Gladstone et al (1998) and the simulation from *FLOW-3D*.

t=0 s

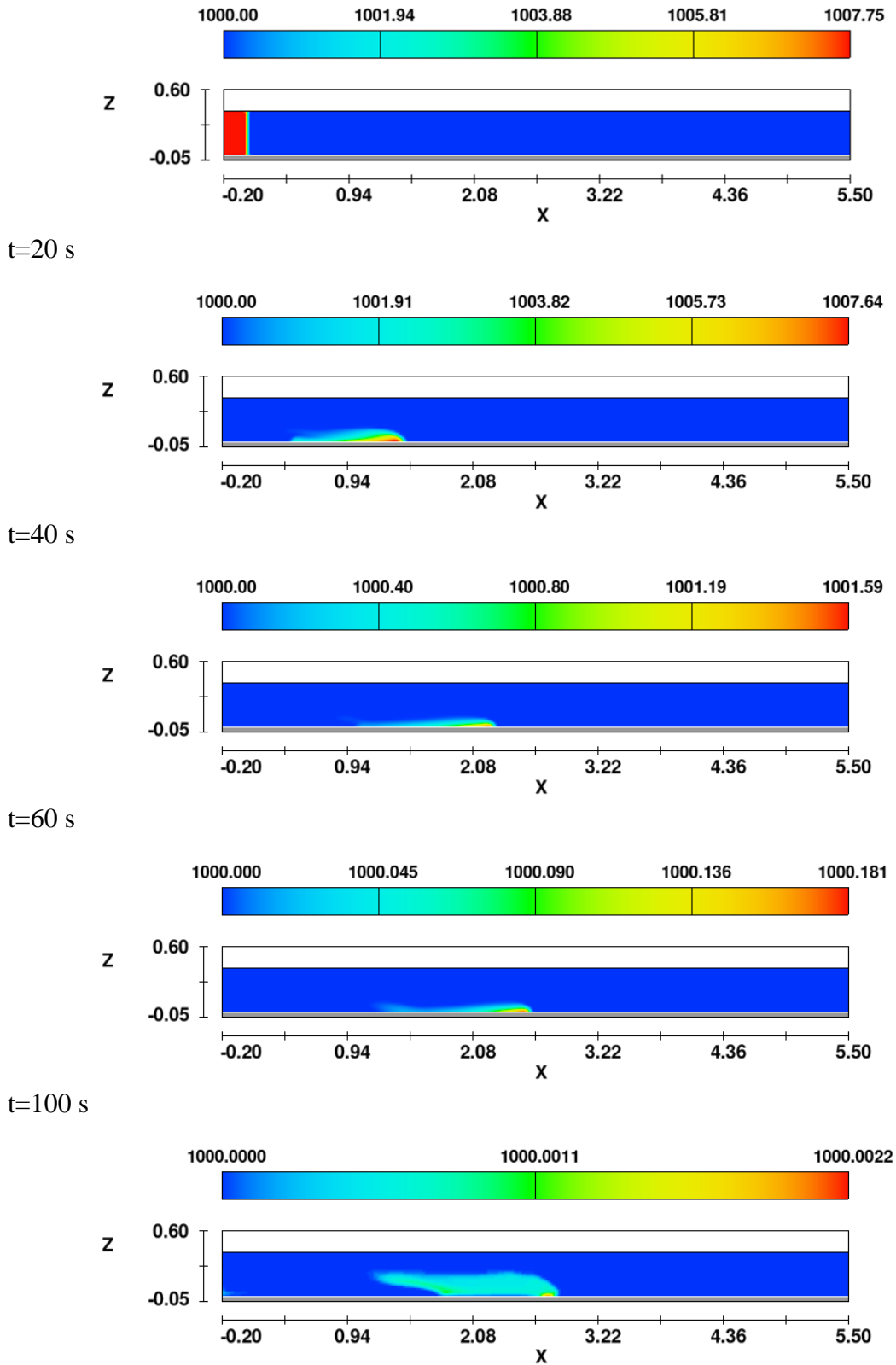


Figure 4. Time variation of density fluid-sediment mixture in the tank.

Figure 4 shows time variation of density of fluid-sediment mixture in the tank for case 1 in Table 1. It is seen that after the lockgate is lifted, the density current causes the sediment to distribute along the length of the tank in the right direction. While flow-front advances, the density of the fluid-sediment mixture decreases due to deposition of the sediment grains. At about 100 s, all the sediment is settled on the bed and the flow-front vanishes.

2) Scour in a flume

Figure 5 shows the experimental flume setup for a submerged horizontal jet in Chatterjee (1994). Water enters the flume at a 1.56 m/s velocity through a narrow slit 2 cm in width. The resulting two-dimensional sheet of water flows over a solid apron, 66 cm in length, before contacting a packed bed of sand 300 cm in length and 25 cm in depth. The median diameter of the sand grains is 0.76 mm. The channel is 60 cm in width, wide enough so that three-dimensional effects can be neglected near the middle of the flume. The scour profiles were measured down the centerline of the flume.

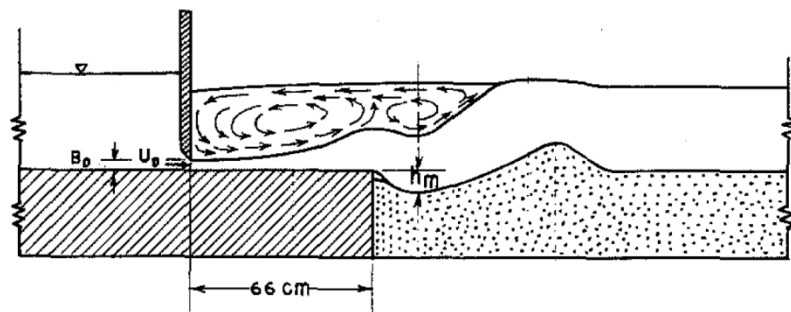


Figure 5. Experimental flume setup for a submerged horizontal jet (Chatterjee et al,1994)

Figure 6 shows the 2D computational domain that is 160 cm long starting the slit and 50 cm high including 15 cm of packed bed. There are 9240 mesh cells in total. In the simulation, the critical Shields parameter is 0.05, both the entrainment and bedload transport coefficient use the default values (0.0018 and 8.0, respectively), and the micro-density of sand is 2.65 g/cm³.

Figures 7 and 8 present the measured and the calculated scour profiles at different time, respectively. It is found the calculated shape and elevation of the sand bed compare well to those measured in the experiment. As measured, a scour hole is generated just behind the apron due to entrainment and bedload transport. Deposition mainly occurs immediately behind the scour hole to form a sand dune. Figure 9 shows time-variations of the maximum scour hole depth and the maximum dune height. Good agreement is observed between the measurement and the calculation. The maximum scour hole depth is only slightly underestimated and the maximum dune height is slightly overestimated.

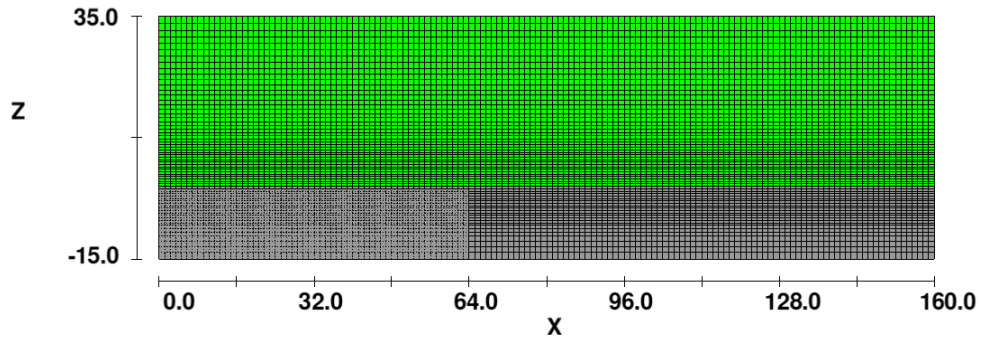


Figure 6. Computational domain and mesh setup to simulate scour in the flume

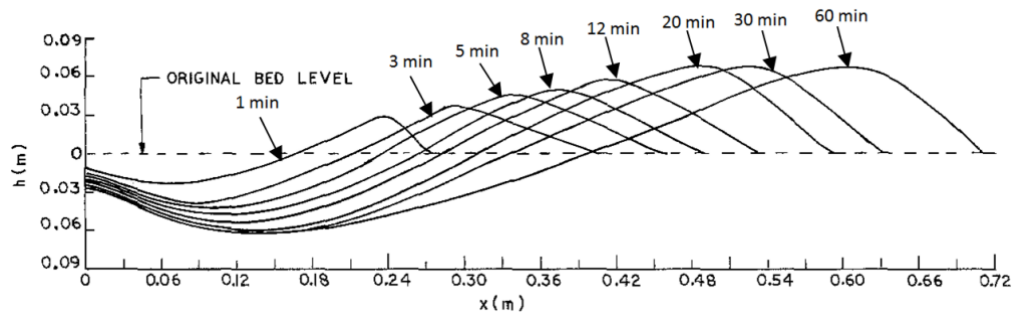
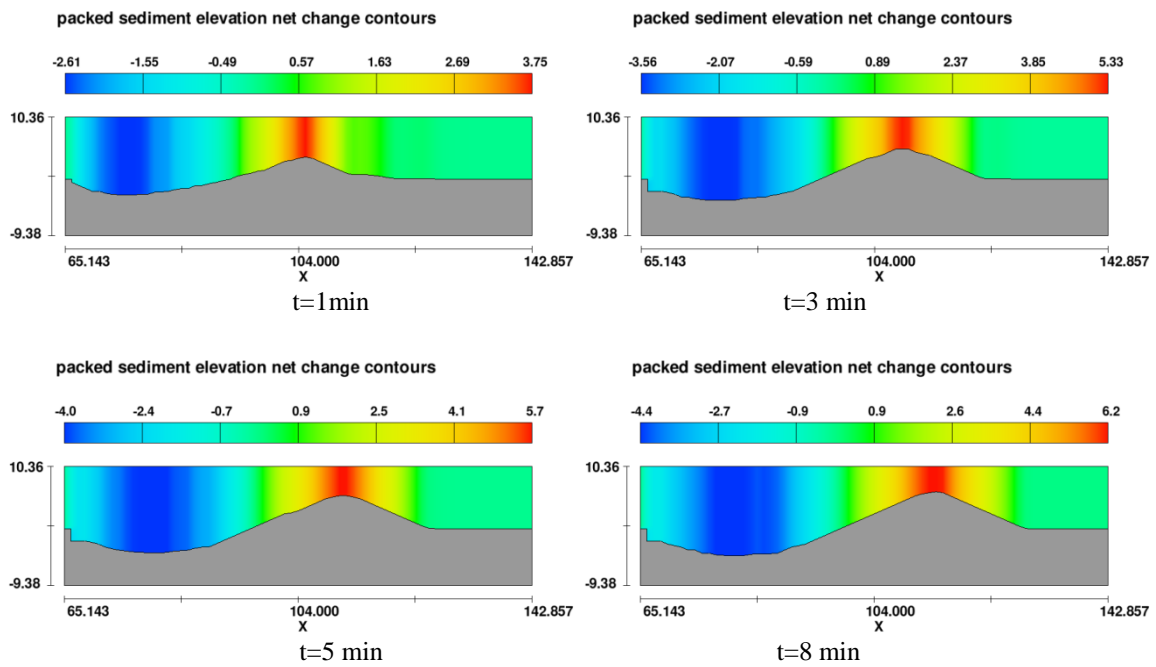


Figure 7. Measured time-variation of packed bed profile (Chatterjee et al, 1994)



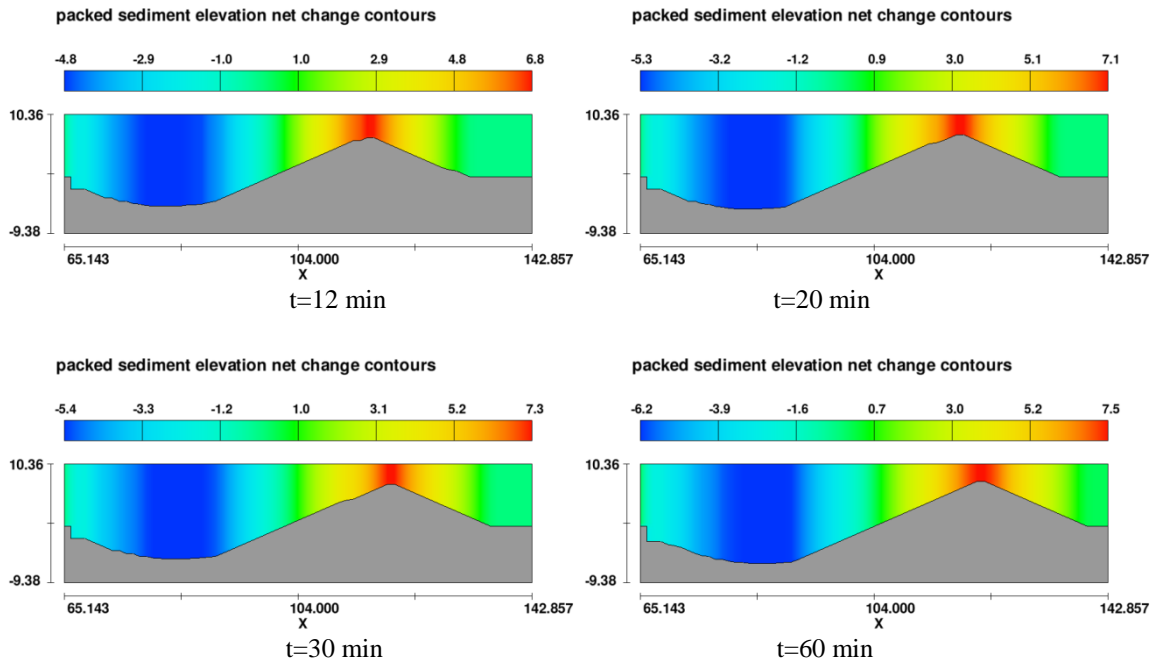


Figure 8. Calculated time-variation of packed bed profile after the apron

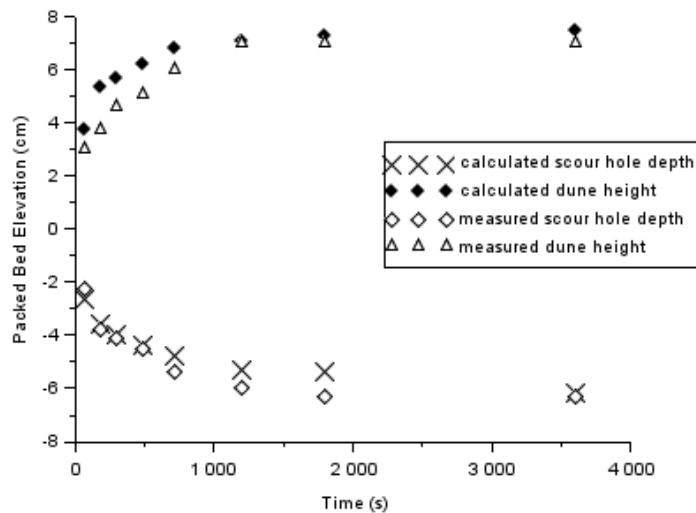


Figure 9. Time variation of maximum scour hole depth and dune height

3) Scour at cylindrical piers

In this case, clear water scour around a row of three cylindrical piers is simulated. The piers are 1.5 m in diameter and spaced by a 2 m distance next to each other. The oncoming flow is aligned with the cylinders and has a 2 m/s velocity. The packed bed is

composed of three sediment species which are fine gravel (5 mm in diameter), medium gravel (10 mm) and coarse gravel (20 mm). All the species have the same mass density and scour parameters: mass density = 2650 kg/cm^3 , critical Shields parameter = 0.05, entrainment coefficient = 0.018, and bedload coefficient = 8.0. The critical packing fraction is 0.64.

Figure 10 shows the computational domain and the mesh setup. Since the problem is symmetric in the lateral direction, the domain covers only the region at one side of the cylinders. The mesh has 367,500 non-uniform cells that are finer close to the cylinders. At the upstream boundary of the mesh block, a velocity profile obtained from a simulation of turbulent flow over a flat plate is used.

Figure 11 shows flow around the cylinders at 8 min. Figure 12 shows the scour holes around the cylinders and their variations with time. Figure 13 shows the net change of the interface elevation, where the negative and positive values represent scour depth and deposition height, respectively. It is seen that a scour hole is formed at the front and two lateral sides of each cylinder, and there is no scour immediately behind it. This is because the flow around a cylinder is accelerated under the favorable pressure gradient after it passes the cylinder's front nose, which results in high bed shear stress in the local region. Immediately behind the cylinder, flow has passed the separation points with its direction reversed and speed reduced due to the adverse pressure gradient, resulting in bed shear stress lower than the critical shear stress. The scour holes are shallower around the middle and the rear cylinders because they are in the wake of the front cylinder.

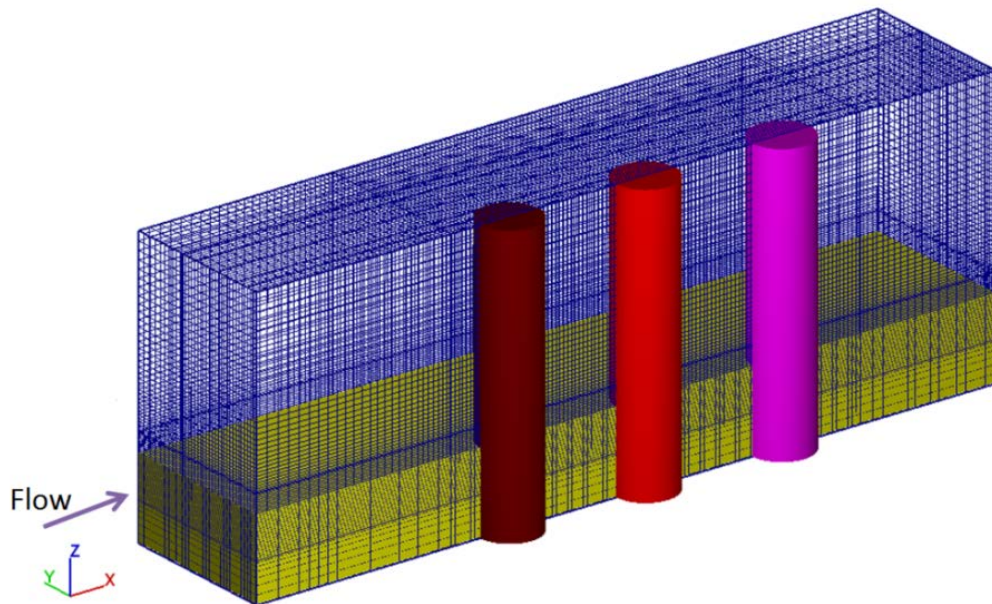


Figure 10. Computational domain and mesh setup around a row of three cylinders

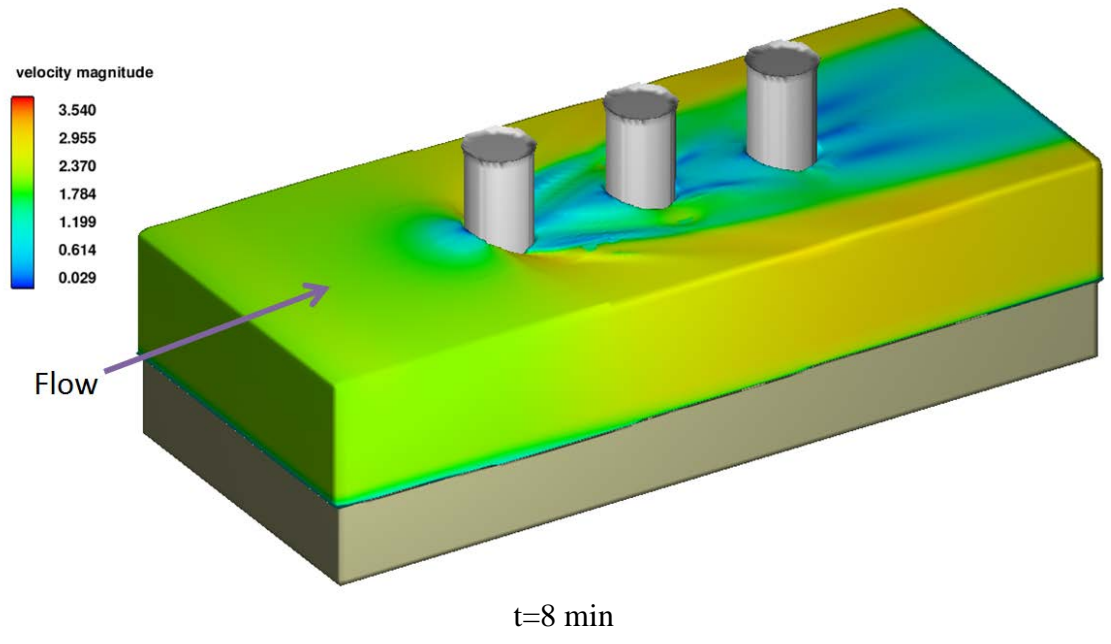
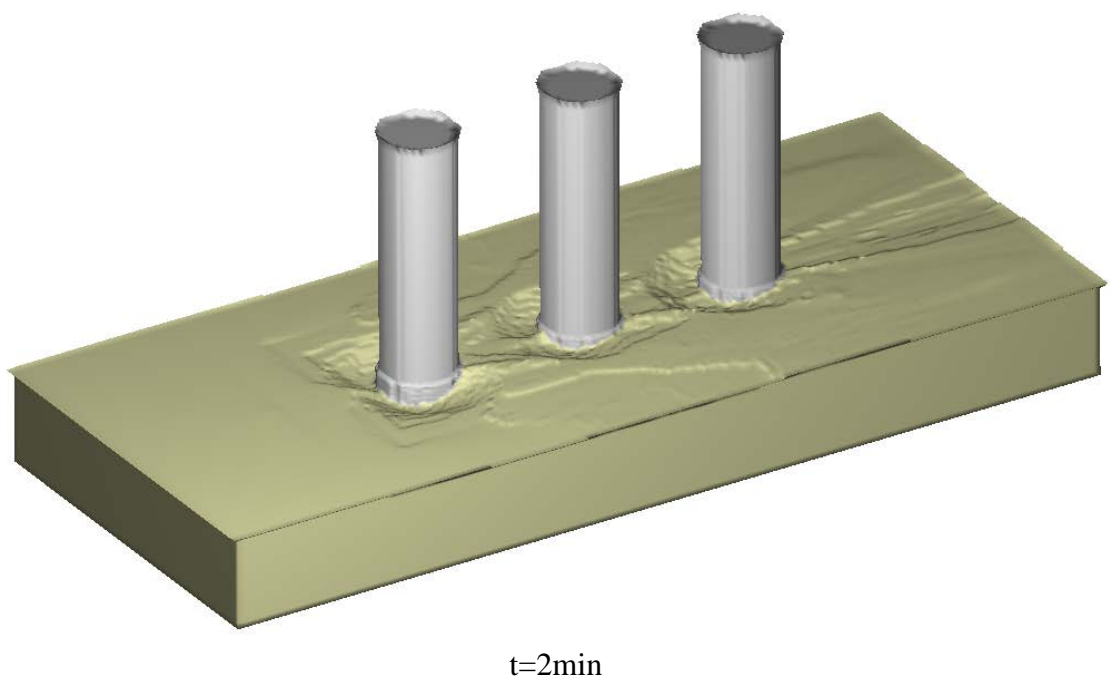
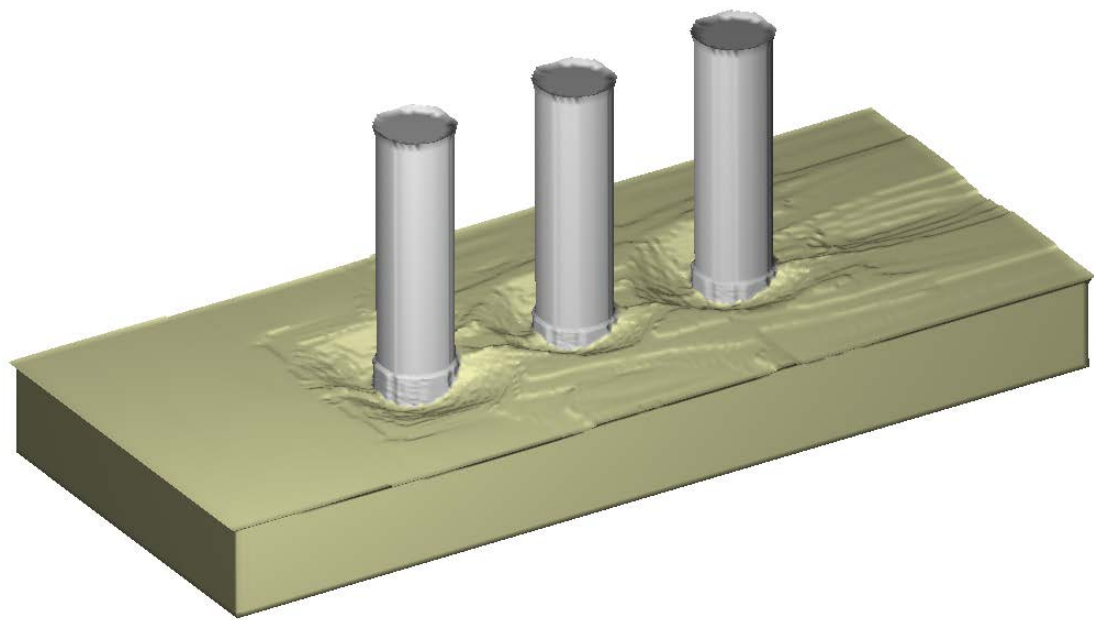
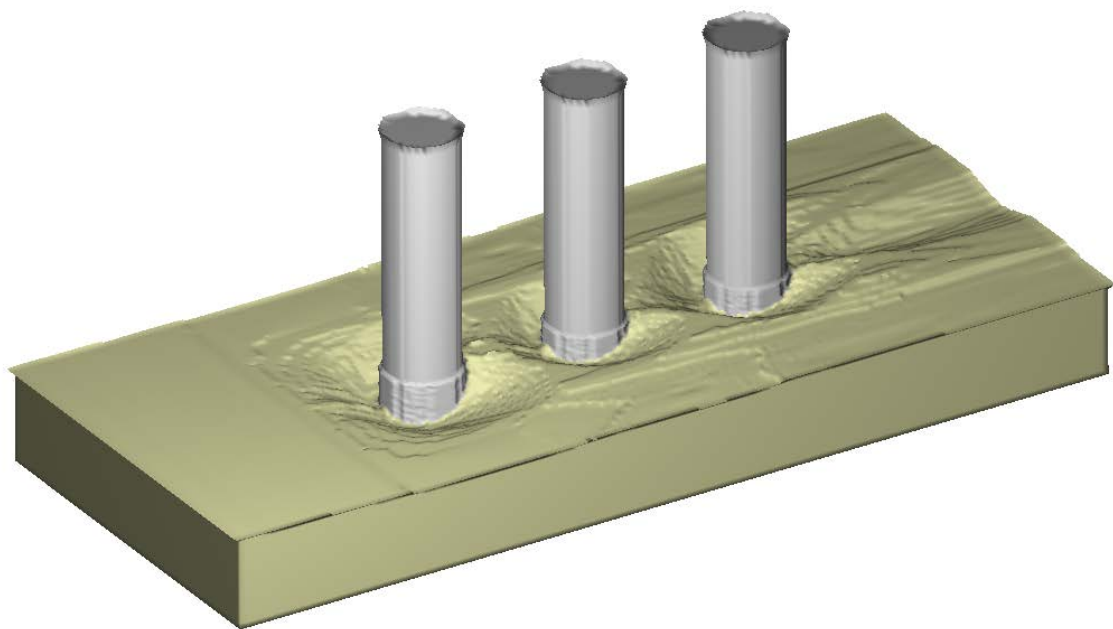


Figure 11. Flow around the three cylinders





t=4min



t=8min

Figure 12. Plots of scour holes around the cylinders at different time

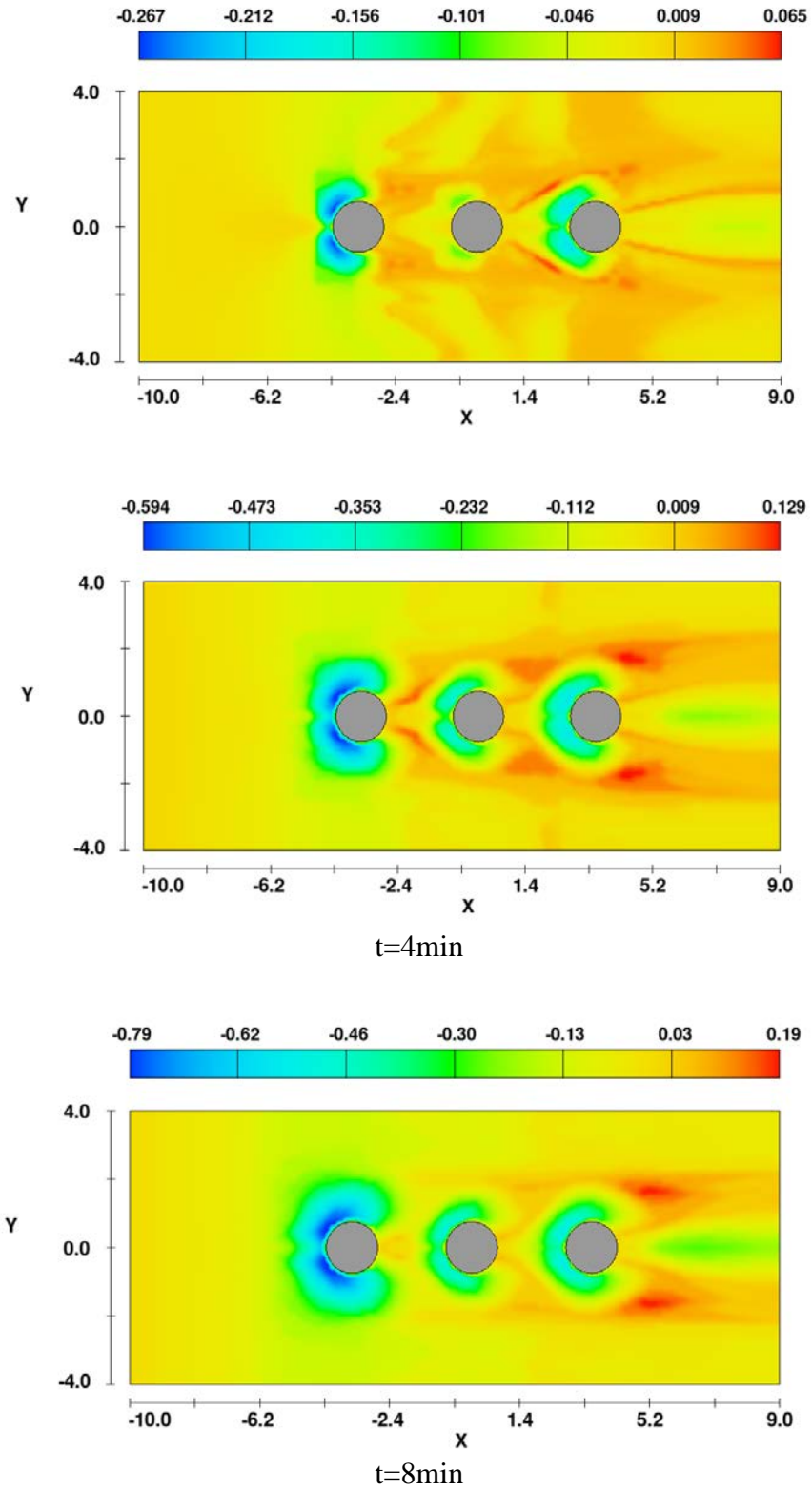


Figure 13. Scour depth (in negative value) and deposition height (in positive value) at different time

4) Full Dam and Spillway Simulation

A more real-world simulation of a full dam and spillway was simulated using the new sediment scour model. This simulation involves the geometry and initial water region shown in Figure 14. The mesh used in this simulation is composed of four mesh blocks, as shown in Figure 15. The mesh block used to define the spillway (in orange) has a uniform mesh size of 0.34m. The two mesh blocks used to define the regions to the right and left of the spillway (in green and blue) have a uniform mesh size of 1.02m, while the mesh block defining the dam itself (in red) has a resolution ranging from 0.6m to 0.78m. The total number of mesh cells is 3,694,508.

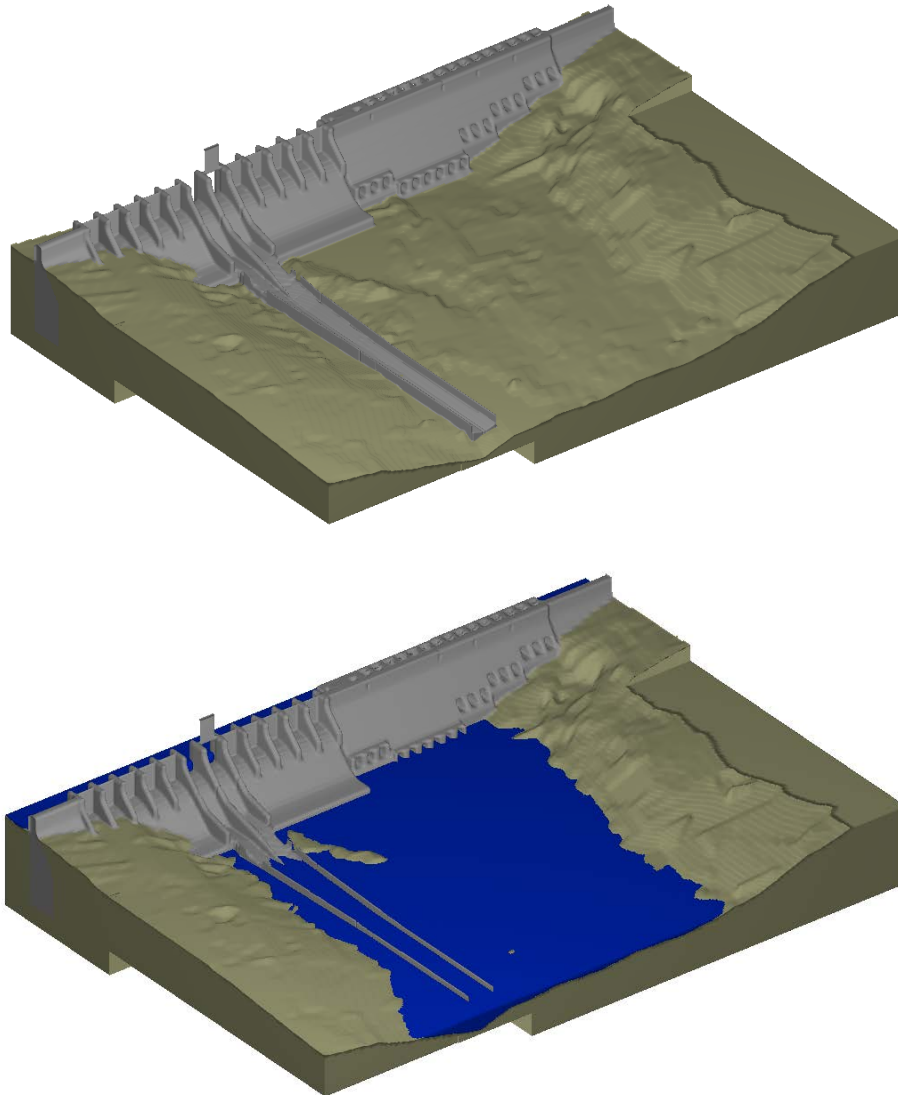


Figure 14: Initial setup of full dam and spillway simulation showing the topography (brown region), the dam structure (grey region) and the initial water region (blue region). The height of the dam from its base to top is 30m.

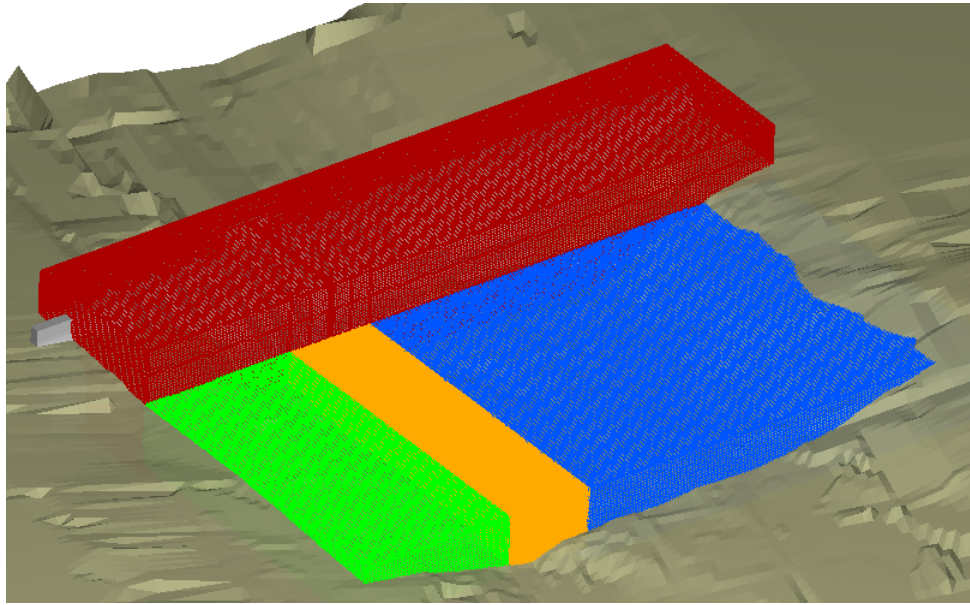
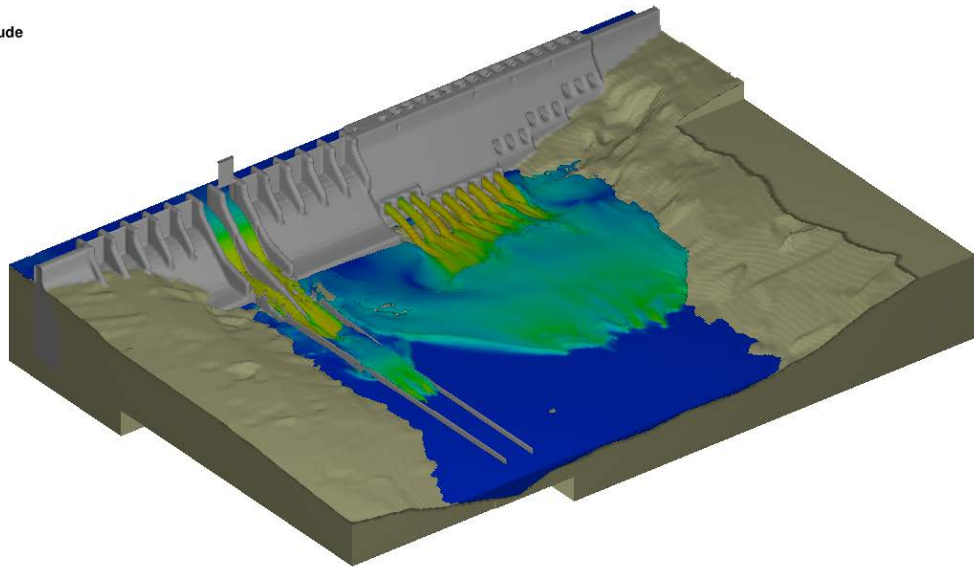
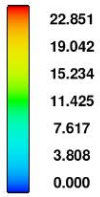


Figure 15. Mesh setup showing the four mesh blocks used to mesh the problem domain.

The topography is composed of a packed sediment mixture of three species in equal proportions: sand ($d=1\text{mm}$), coarse sand ($d=2.5\text{mm}$) and gravel ($d=10\text{mm}$). All the species have the same microscopic density, 2650 kg/m^3 . The critical packing fraction is 0.64, and the default values of the entrainment and bedload coefficients were used, 0.018 and 8.0, respectively. The critical Shields parameter is 0.05.

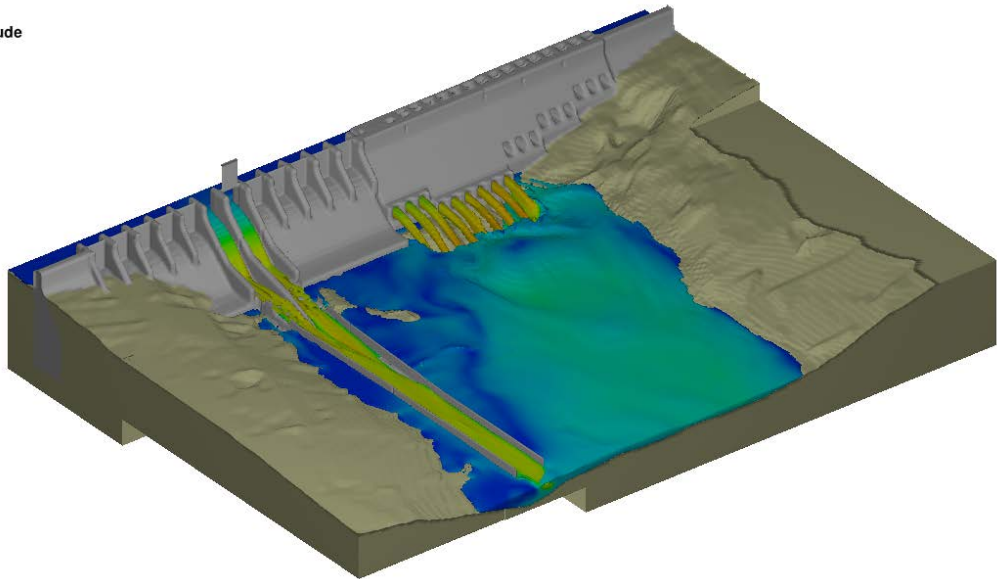
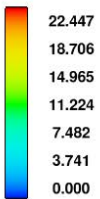
In the simulation, water flows through both the spillway and through the outlet pipes of the dam (to the right of the spillway in Figure 14). Figure 16 shows a time-series plot of the water flow in the simulation. Figure 17 shows a time-series plot of the packed bed interface. There are two regions where the water flow is the greatest – over the spillway and through the outlet pipes, and flow speed is higher than 20 m/s. Because the spillway has a concrete lined channel, the erosion in this vicinity is minimal. Downstream of the outlet pipes there is locally high shearing and turbulence; it is in this area that erosion is the greatest. Figure 18 presents variation of scour depth (in negative value) and deposition height (in positive value) with time. The deepest scour depth downstream of the outlet pipes increases rapidly to 2.2 m, 9.0 m and 11.1 m after 10 s, 50 s and 100 s of time. Obvious deposition occurs in the region between the spillway and the main stream from the outlet pipes because of the local flow is slow such that the tendency of deposition exceeds that of entrainment. At the right side of the water region there exists a tiny deposition area (circled with blue color in Figure 18) due to sliding of a steep slope of packed grains.

velocity magnitude

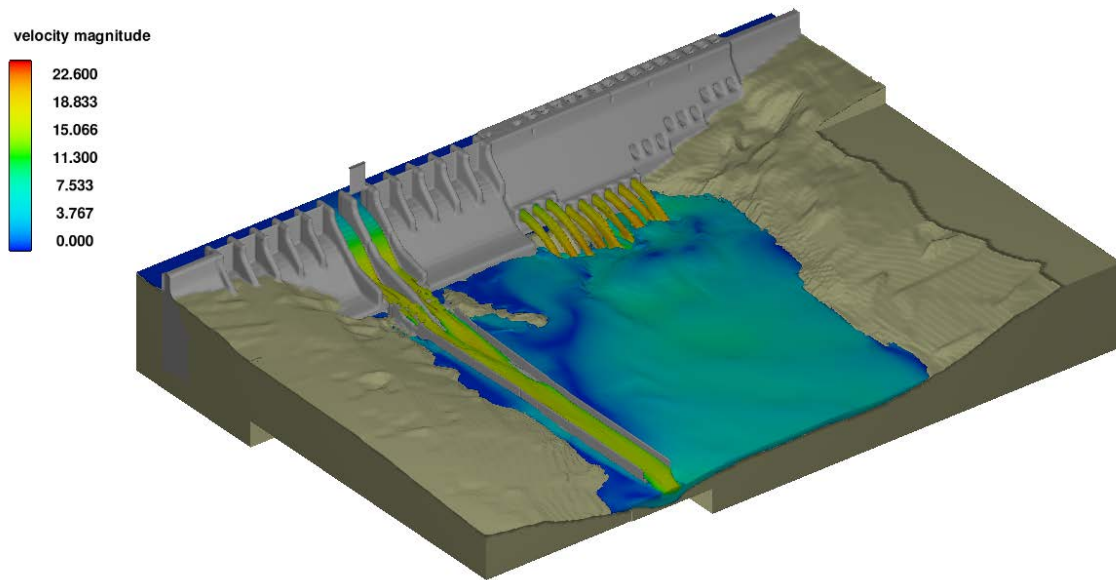


t=10s

velocity magnitude

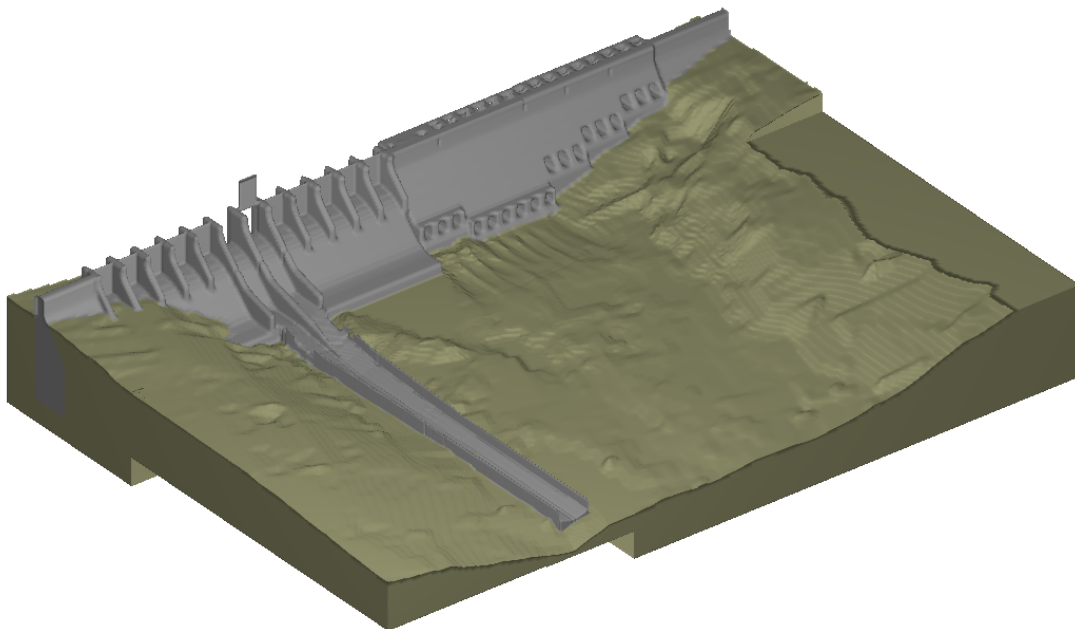


t=50s

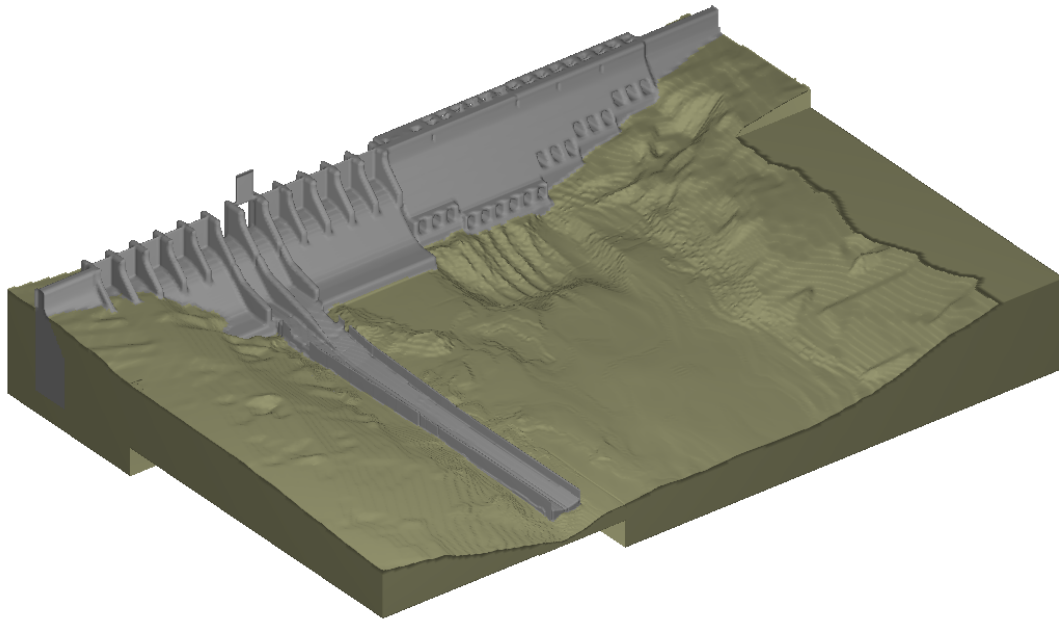


t=100s

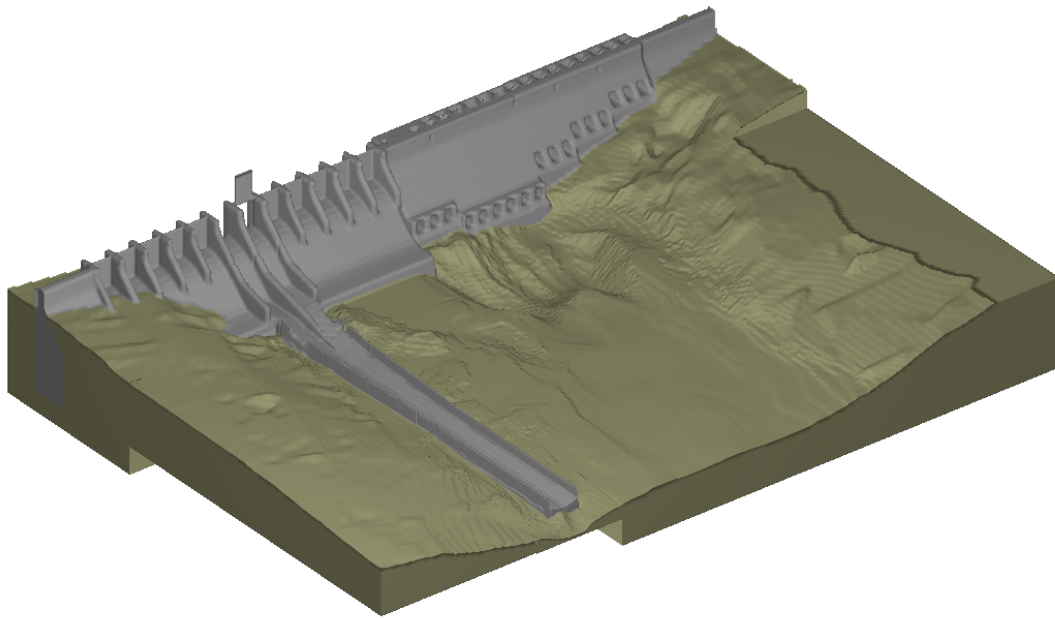
Figure 16: Time evolution of the water flow in the full dam and spillway simulation.



t=10s



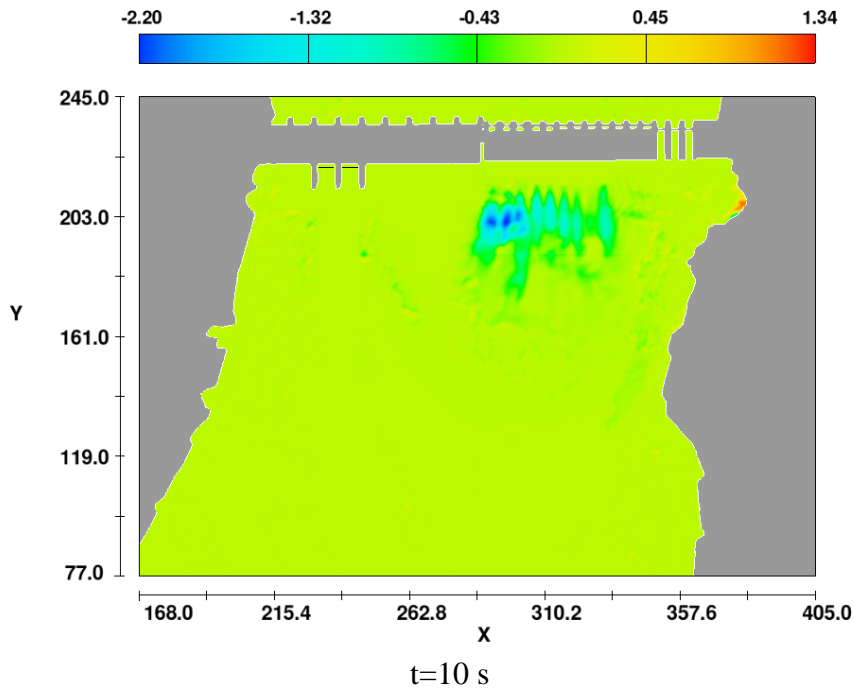
t=50s



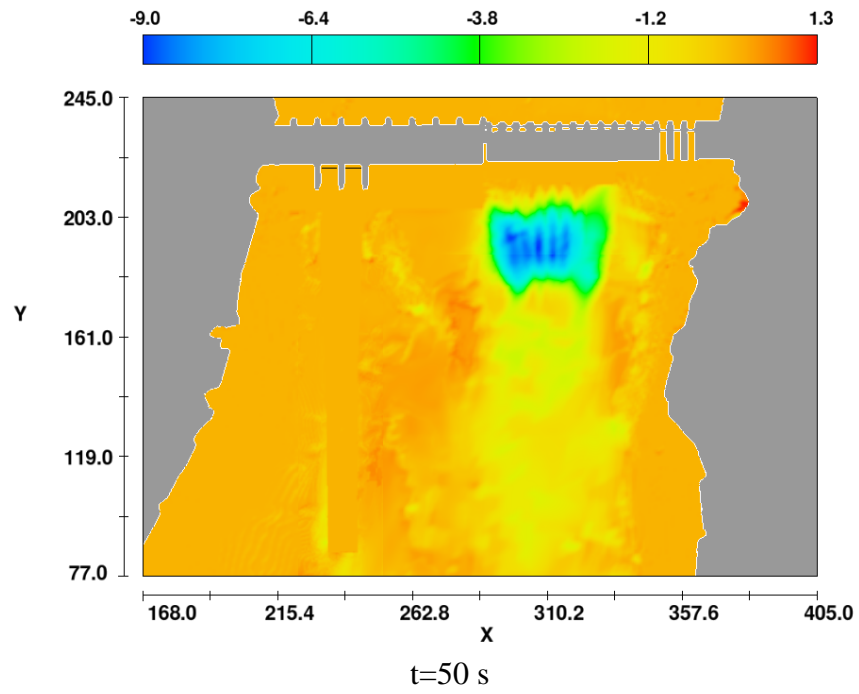
t=100s

Figure 17: Variation of the packed bed surface with time

packed sediment elevation net change contours



packed sediment elevation net change contours



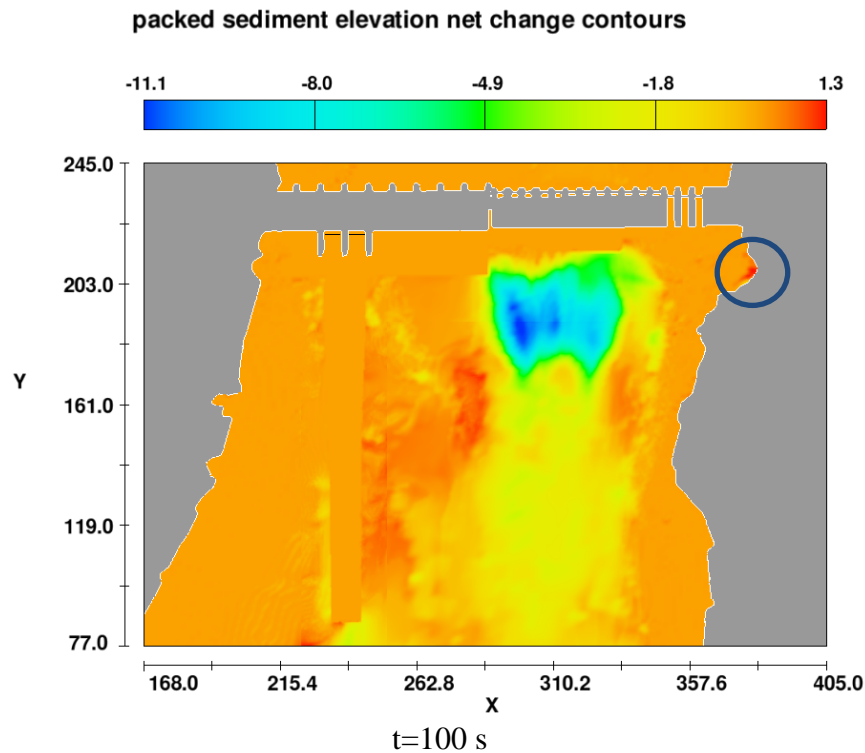


Figure 18. Variation of scour depth (in negative value) and deposition height (in positive value) with time

5) Scour with shallow water flow

In this shallow water simulation, clear water flows into an initially flat and dry channel at a velocity of 1.0 m/s, as shown in Figure 19. The bed material is coarse sand with 2 mm in grain diameter and 2650 kg/m^3 in density. The horizontal lengths of the channel in x and y are 2 km and 1 km, respectively. Initial water depth at the upstream boundary is 5 m. The ratio of the depth to the horizontal length of the flow is in the order of 10^{-2} thus satisfies the criteria for shallow water flow. There are 100×50 cells in the mesh shown in Figure 19.

Figure 20 shows the calculated time variation of water velocity distribution. The strongest flow (higher than 4 m/s) is found in the downstream region where the channel is not only narrow but also has a sharp turn. Figure 21 shows variation of scour depth (in negative value) and deposition height (in positive value) with time. As expected, erosion is strong in the fast flow regions. The greatest scour depth is found just at the fastest flow location, which is 3.82 m, 7.0 m and 10.1 m after 30 min, 60 min and 120 min, respectively. Deposition up to 2.9 m is observed in the slow flow regions because the settling velocity exceeds the lifting velocity of the sand grains due to low bed shear stress.

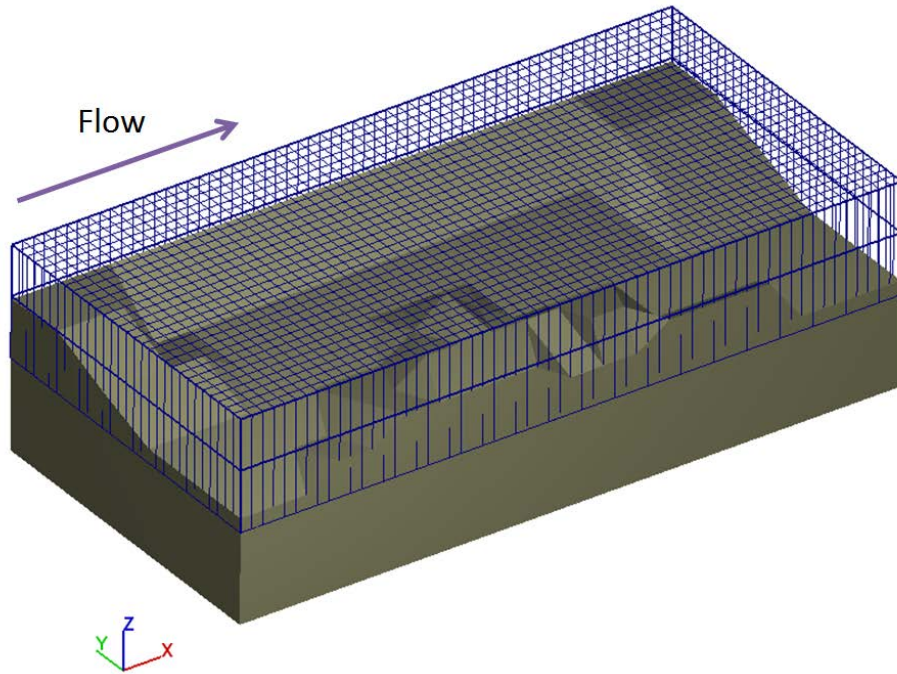
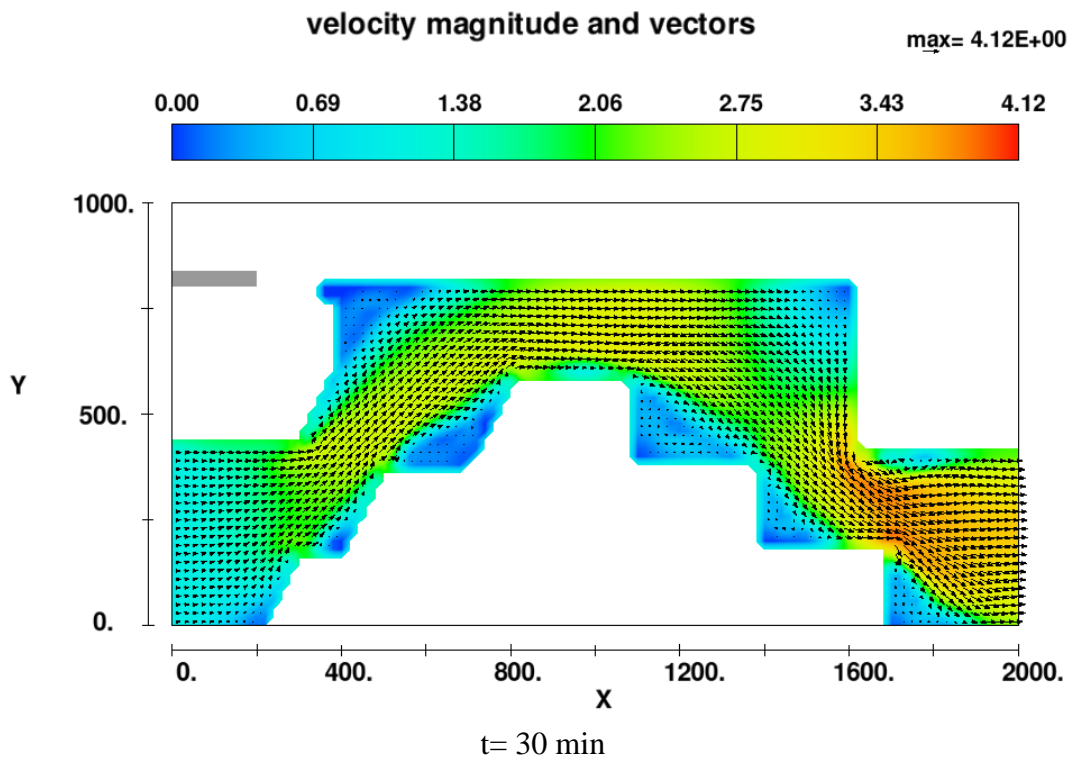


Figure 19. Computational domain and mesh setup



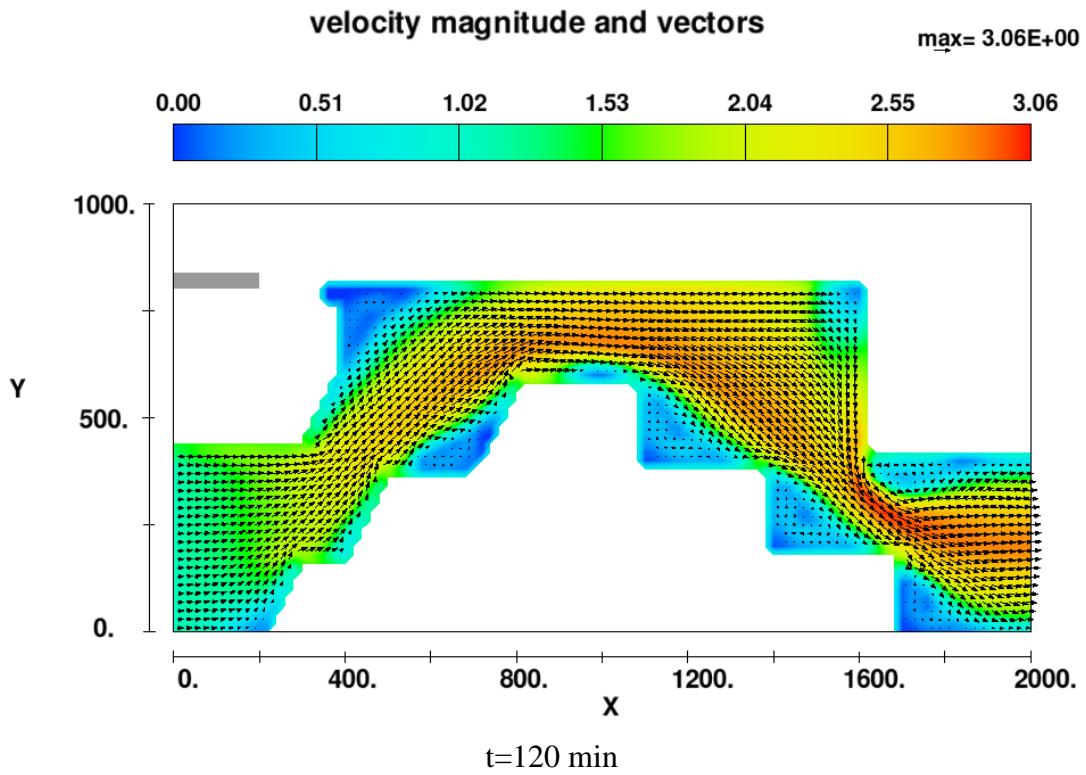
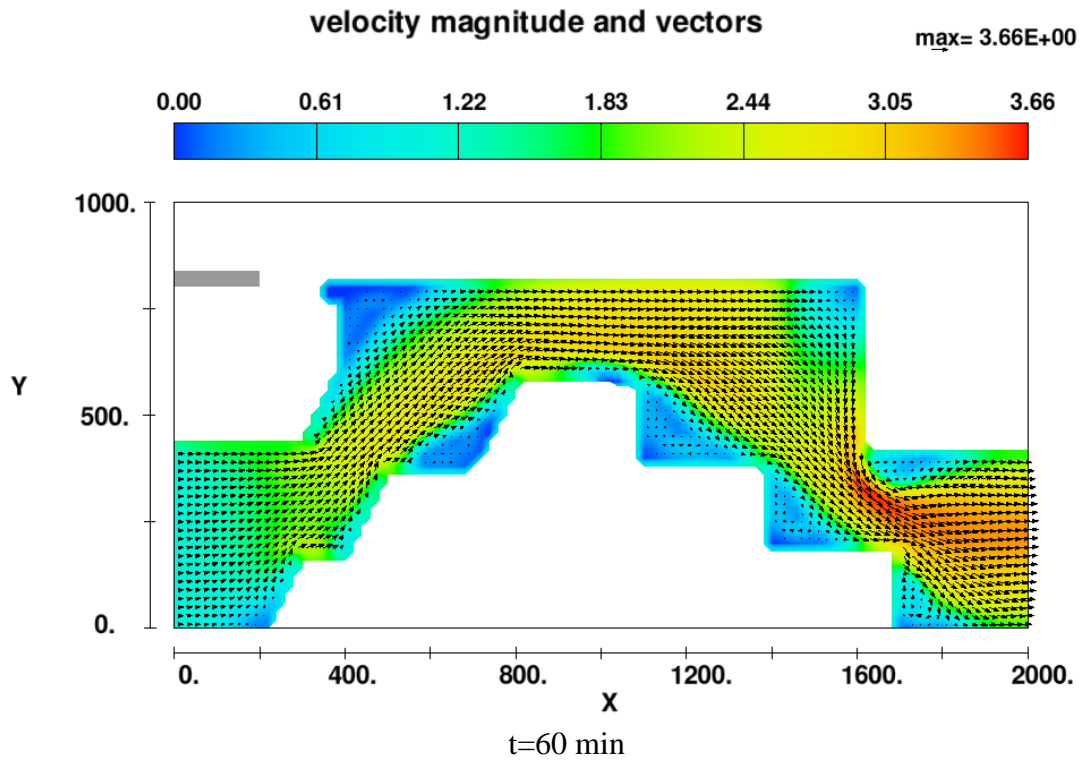
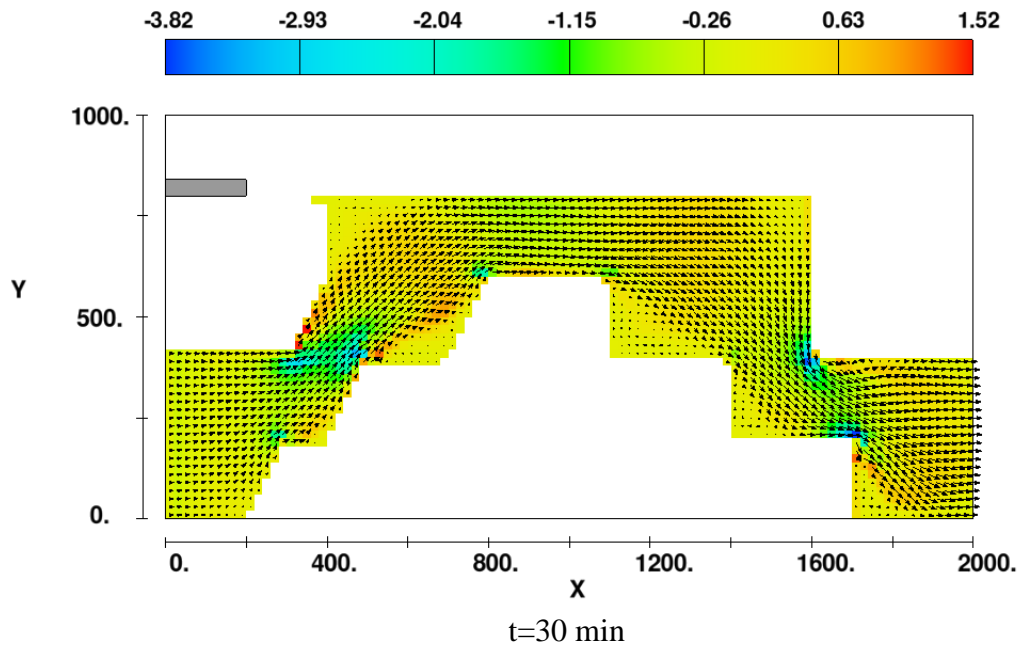


Figure 20. Distribution of water velocity versus time

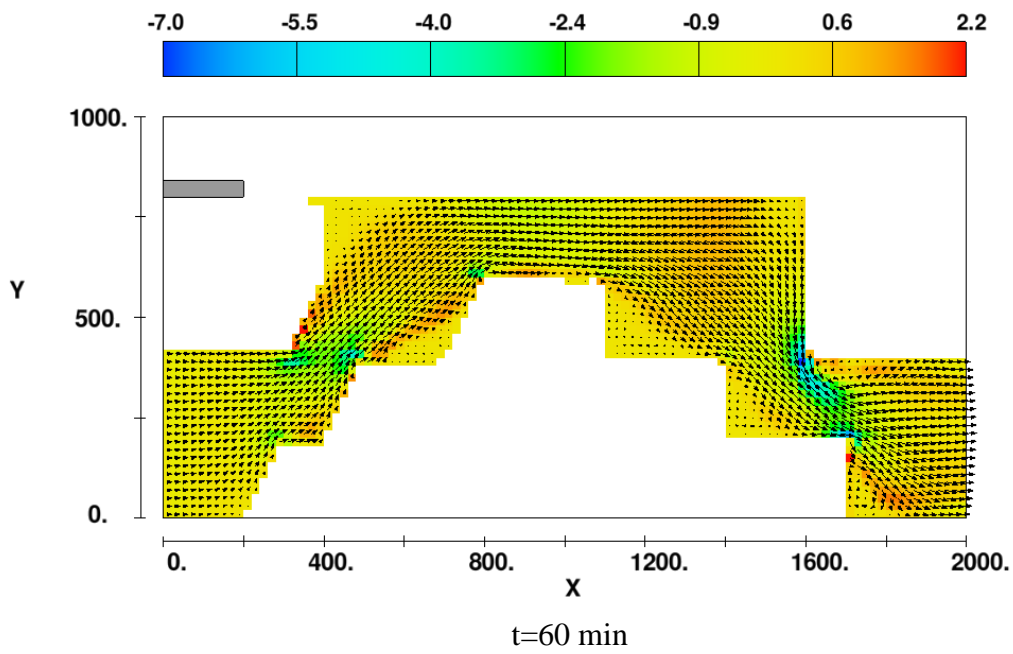
packed sediment elevation net change and vectors

max= 4.12E+00



packed sediment elevation net change and vectors

max= 3.66E+00



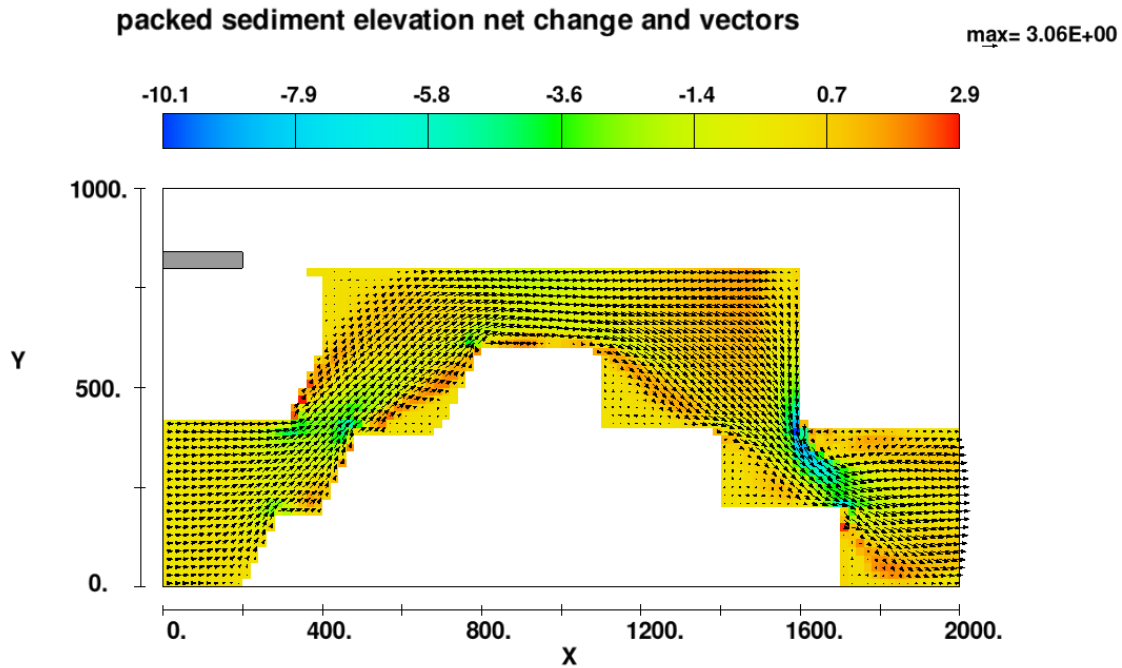


Figure 21. Distribution of scour depth (in negative value) and deposition height (in positive value) versus time

5. Conclusions

Fully-coupled with fluid dynamics, the sediment scour model in *FLOW-3D* simulates all the sediment transport processes of non-cohesive soil including bedload transport, suspended load transport, entrainment and deposition. It allows multiple sediment species with different properties including grain size, mass density, critical shear stress, angle of repose, and parameters for entrainment and bedload transport. The model works for both 3D flows and 2D shallow water flows.

In the model, the packed sediment bed is defined by one geometry component that can be composed of multiple subcomponents with different combination of sediment species. It is modeled with the FAVORTM technique which uses area and volume fractions for a far more accurate representation of the packed bed interface than was used in earlier versions of *FLOW-3D*. In the mesh cells containing the bed interface, location, orientation and area of the interface are calculated and used to determine the bed shear stress, the critical Shields parameter, the erosion rate and the bedload transport rate. Bed shear stress in 3D turbulent flow is evaluated using the standard wall function with consideration of the bed surface roughness that is proportional to the media grain size d_{50} . For 2D shallow water flows, the bed shear stress is calculated following the quadratic law where the drag coefficient is either user-defined or locally calculated using the water depth and the bed surface roughness related to the local median grain size d_{50} .

The model calculates bedload transport using a sub-mesh method based on the equation of Meyer-Peter and Muller (1948). Suspended sediment concentrations are obtained by solving the sediment transport equations. Computation of erosion considers sediment entrainment and deposition simultaneously. The lifting velocity of grains in entrainment follows the equation of Winterwerp et al. (1992). The settling velocity is calculated using an existing equation in Soulsby (1997) for deposition and suspended load transport.

Model validations were conducted for two cases: scour in a flume where sand was eroded by a submerged horizontal jet; and deposition in a long tank where the initially existing suspended sediment in the rectangular region at one end of the tank distributes to the whole tank. In the former, the calculated time variations of sand bed profile, the maximum scour depth and the maximum dune height match well with the experimental result. In the latter, a good agreement between the calculated and measured distribution of deposit density is achieved. The model was also applied to scour around a row of three piers, scour at a dam and scour in a channel and obtained reasonable results. The capability of the model to simulate scour in real world problems was successfully demonstrated.

The model has limitations. It does not work for cohesive soils such as silts and clays. Caution should be taken when it is applied with excessively large grains due to the limited validity of the sediment theory used in the model. Due to the empirical nature of the sediment theory and other approximations such as those in the turbulence models, parameter calibration may be needed in applications to achieve the best results.

References

- Chatterjee, S. S., Ghosh, S. N., and Chatterjee M., 1994, Local scour due to submerged horizontal jet, *J. Hydraulic Engineering*, 120(8), pp. 973-992.
- Brethour J., 2003, Modeling Sediment Scour, Technical note FSI-03-TN-62, Flow Science.
- Brethour, J. and Burnham, J., 2010, Modeling Sediment Erosion and Deposition with the *FLOW-3D* Sedimentation & Scour Model, Technical note FSI-09-TN-85, Flow Science.
- Gladstone, C., Phillips, J. C. and Sparks R. S. J., 1998, Experiments on bidisperse, constant-volume gravity currents: propagation and sediment deposition, *Sedimentology* 45, pp 833-843,
- Meyer-Peter, E. and Müller, R., 1948, Formulas for bed-load transport. Proceedings of the 2nd Meeting of the International Association for Hydraulic Structures Research. pp. 39-64.
- Soulsby, R., 1997, Dynamics of Marine Sands, Thomas Telford Publications, London.

- Soulsby, R. L. and Whitehouse, R. J. S. W., 1997. Threshold of sediment motion in Coastal Environments. Proc. Combined Australian Coastal Engineering and Port Conference, EA, pp. 149-154.
- Van Rijn, L. C., 1984, Sediment Transport, Part I: Bed load transport, Journal of Hydraulic Engineering 110(10), pp 1431-1456.
- Winterwerp, J. C., Bakker, W. T., Mastbergen, D. R. and Van Rossum, H., 1992, Hyperconcentrated sand-water mixture flows over erodible bed. J. Hydraul. Eng., 118, pp. 1508–1525.